

# Microwave Imaging of Composite Materials Using Image Processing

Azadeh Noori Hoshyar, Sergey Kharkovsky, Bijan Samali

Institute for Infrastructure Engineering  
Western Sydney University  
Penrith, Australia

Azadeh.H@westernsydney.edu.au, s.kharkivsky@westernsydney.edu.au, B.Samali@westernsydney.edu.au

**Abstract**— This paper presents the results of application of a relatively simple microwave continuous wave reflectometer with an open-ended waveguide antenna for the purpose of nondestructive testing and evaluation of composite materials using their images. It is shown that the resulting original images could not reveal a desired amount of information about the interior of the sample under investigation and the proposed image processing techniques can improve the results in particular as it relates to detecting the targets located at different depths. This paper presents the results of this investigation and a discussion of these results.

**Keywords**— *microwave imaging; open-ended rectangular waveguide antenna; composite materials; construction materials; image processing; segmentation*

## I. INTRODUCTION

The health monitoring of materials is the crucial concern in all areas of engineering to avoid the degradation risks caused by defects. These defects can worsen over time due to various reasons. The inspection, diagnosis and maintenance are the important factors to identify the early detection and repair of defects and lead to the prediction of life span of such structures. Since these investigations are performed by expert inspectors, the process is time consuming, expensive and subjective. Therefore, automated defect detection systems based on image processing approaches are desired [1].

In such automatic systems, the selection of appropriate imaging techniques is of high priority. Microwave imaging is the technique applied to sense a given object by means of examining microwave pulses or continuous wave signals. This technique offers comprehensive descriptions for the imaging systems. Microwave or millimeter wave imaging systems have been used for medical applications, security scanning, and nondestructive testing and evaluation (NDT&E) of various metal, dielectric, and composite materials [2-6]. However, to obtain desired range resolution and 3D images, the relatively complex wide frequency range measurement systems and image algorithms are required. In many applications including the NDT&E, wide band techniques may not be applicable due to specific requirements, e.g., depth of penetration in composite materials and cost of the techniques.

In this paper a relatively simple continuous wave reflectometer is used along with an open-ended waveguide

antenna (OEWA) to obtain the magnitude and phase of the microwave reflection coefficient at single frequencies. The resulting original images could not reveal a desired amount of information about the sample under tests. Therefore, in this paper image processing algorithms are proposed to be applied on the obtained data for improving the images. The researchers and engineers are spending much time and effort to propose and employ suitable image-based algorithms for automatic controllers due to the growing concern of degradation conditions in structures. Tanaka et al. [7], developed a patented system to use as structural inspector for bridges. They employed wavelet transform in their algorithm. Abdel-Qader et al. [1] performed a comparative study on crack detection on the bridge surface by employing the wavelet transform, Fourier transform, Sobel filter, and Canny filter. The comparison of the results show the better performance of wavelet transform than the others. In another research [8], the wavelet transform and Canny edge detection methods have been employed for the purpose of crack detection in a concrete structure. Some researchers [9, 10] employed the morphological image processing in their detection systems. P. Cotič et al. [11] proposed the fusion of ground penetrating radar (GPR) data, thermographic phase data and improving the visualization of defects in concrete using the fuzzy c-mean algorithm. In this paper, three different algorithm-based solutions based on Fourier transform, wavelet transform and fuzzy c-mean to facilitate the structural damage identification are proposed and applied to microwave images of composite materials.

The rest of this paper is structured as follows: The measurement approach and specimens are described in Section II. In Section III, the proposed image processing algorithms for defect detection are explained in detail. The results are demonstrated in Section IV, and Section V is assigned to conclusion.

## II. MEASUREMENT APPROACH AND SPECIMENS

### A. Measurement Approach

In this investigation the OEWA's were used at single frequencies. The OEWA's are robust, reliable, efficient and relatively simple antennas. The complex microwave reflection coefficient over a plane for each sample was measured using a commercial Agilent performance network analyzer (PNA) and a custom-made scanning imaging system [12]. The antenna irradiated the sample under test and picked up the signal reflected from the sample. Data was acquired by using a PNA

where the magnitude and phase of the microwave reflection coefficient was recorded for every data point. Images of the panel were generated using the data and the proposed image processing algorithms.

### B. Specimens

To highlight the utility of the single-frequency reflectometer with the OEWA along with the proposed image processing approaches for imaging of composite materials a few samples were prepared and imaged.

One of the samples with dimensions of 240 mm by 240 mm by 90 mm (referred to as Sample 1 here) consisted of 6 equally-thick layers of construction foam, as shown in Fig. 1(a). Four metal discs (each of diameter of 25 mm and thickness of 2 mm) in two groups of two were placed at interfaces between layers 1–2, and 5–6, respectively, as shown in Fig. 1(c)-(d). In this paper the results for this sample will be demonstrated. Sample 1 was scanned with a 3 mm-step size (along x- and y-axes), while the complex reflection coefficient was measured at frequency of 11.5 GHz (X-band) and at the standoff distance of 30 mm (the distance between the OEWA aperture and the top surface of Sample 1). The data for other samples such as dielectric-metal layered structures possessing metal surface defects have been obtained at different frequencies and image processing for these samples is in progress.

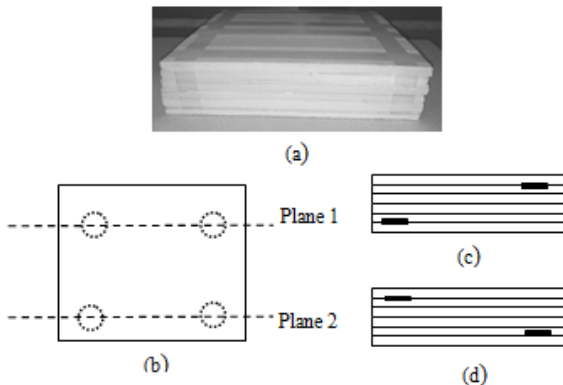


Fig 1. Sample 1: (a) picture and schematic of (b) top view with indication of embedded disks, (c) cross-sectional side view at Plane 1 and (d) cross-sectional side view at Plane 2.

### III. THE PROPOSED IMAGE PROCESSING APPROACH

Since the original images of sample 1 are not clear and have low resolution as will be shown later, some effective approaches have been investigated to achieve the enhanced images and segmenting the area of defect. Since luminance of image is very crucial to distinguish the visual features, and the purpose here is to obtain the high level variations between intensities to detect the edges of defect, it would be optimal to convert the image into greyscale in which the minimum intensity value is equal to 0 and the maximum intensity value is equal to 255. Fourier transforms (FT), as one of the most fundamental tools in image processing and analysis, is appropriate for grey level images [13]. In Fourier transform, the convolution property is the most crucial property; as it helps to develop the performance of inverse Fourier transform.

The wavelet transform [14] and Gaussian filtering are adopted as the bases of Fourier transform. These bases convolved in a single and cyclic basis by the Fourier transform of image to compare the reconstructed images. Concerning the Fourier transform of the image, the major points have been demonstrated in the following. In respect to the measured phase and magnitude of reflection coefficient, firstly, a complex sequence is produced by all the magnitudes being equivalent to one, while the phases distributed uniformly through  $[-\pi, +\pi]$ . On the second experiment, a complex sequence is produced by all the phases being equal to zero, while the magnitudes are random.

Since the number of clusters is 3 in this paper because the defect images are expected to be clustered into less or equal to 3 parts consisting the background (material), defect, and possible extra parts, the Multi-thresholding is run by choosing three threshold values. The last step is to perform morphological operation (erosion) to clean the extra parts.

Algorithm 1 and 2 shows the first and second proposed procedure of defect segmentation.

**Input:** Phase and Magnitude

**Output:** True target segmentation

1. Compute the basis of Fourier transform on the input as 'y'
  - **Wavelet transform** (*Algorithm 1* employs only this basis in its process)
  - **Gaussian filter** (*Algorithm 2* employs only this basis in its process)
2. Compute the Fourier transform of input as 'x'
3. Single and cyclic convolution of sequences 'x' and 'y'
4. Compute the inverse Fourier transform to get the resulting image 'I'
5. Compute Multi-thresholding on image 'I'
6. Perform morphological operation on the resulted image.

Algorithm 1 and 2. Proposed FT-based algorithms of defect segmentation

Algorithm 3 shows the third proposed procedure of defect segmentation in which the fuzzy c-mean (FCM), as a powerful tool of clustering, has been employed to perform clustering and then morphological operation (erosion) is performed to remove the extra parts.

**Input:** Phase and Magnitude

**Output:** True target segmentation

1. Compute the fuzzy c-mean threshold of input as 't'
2. Compute the fuzzy c-mean clusters of input using 't'
3. Compute Multi-thresholding on the resulted image
4. Perform morphological operation.

Algorithm 3. Proposed FCM-based algorithm of defect segmentation

#### IV. RESULTS

The original images of Sample 1 are shown in Fig.2. It is clear from Fig.2 that the raw images do not provide much observable information.

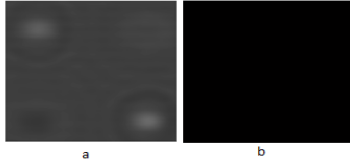


Fig 2. Original image of Sample 1: a) magnitude and b) phase.

In order to enhance the indications of desired targets, three proposed algorithms have been run using the same condition. The first algorithm is the singular and cycling convolution of the wavelet transform as basis of Fourier transform of image followed by the multi-threshold segmentation method and morphological operation ‘erosion’ to remove the extra elements from the image to achieve the targets. Fig. 3 demonstrates the total process of this target segmentation. The first row of images in Fig. 3 shows the process performed by single convolution of the wavelet and Fourier transform. The second and third rows show the process performed by two and three times convolution of the wavelet and Fourier transform. Row one among three rows of Fig. 3 is observable as the best segmented result in Fig. 3.

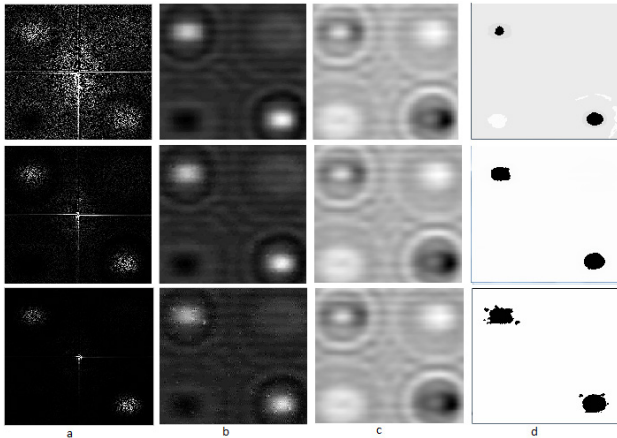


Fig. 3. Images of Sample 1 showing the total process of target segmentation using Fourier transform with the wavelet base followed by Multi-thresholding and erosion, a) Fourier transform b) inverted Fourier transform (magnitude), c) inverted Fourier transform (phase) and d) segmented result.

Fig. 4 shows the results achieved by the second algorithm. It indicates the total process for the singular and cycling convolution of Gaussian as basis of Fourier transform of image followed by multi-threshold segmentation method and morphological operation ‘erosion’ to remove the extra elements from the image to achieve the target. The first row of images in Fig. 4 shows the process performed by single convolution of the Gaussian and Fourier transform. The second and third row of images show the process performed by two and three times convolution of Gaussian and Fourier transform. Row two among three rows of Fig. 4 is observable as the best segmented result in Fig. 4.

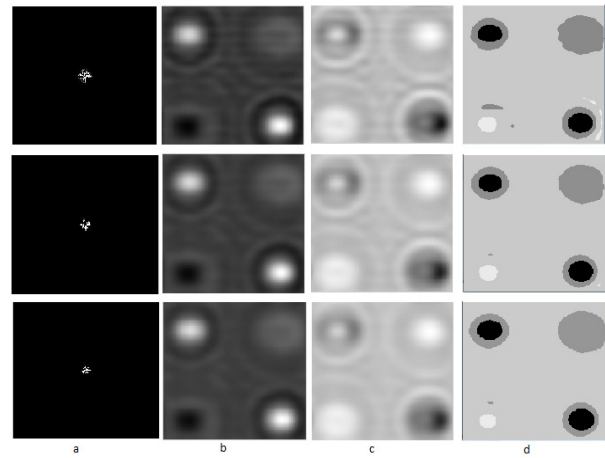


Fig 4. Images of Sample 1 showing the total process of target segmentation using Fourier transform with the Gaussian base followed by Multi-thresholding and erosion, a) Fourier transform b) inverted Fourier transform (magnitude), c) inverted Fourier transform (phase) and d) segmented result.

Fig. 5 shows the results achieved by the algorithm 3. It shows the total process of target segmentation using fuzzy c-mean clustering followed by Multi-thresholding and erosion by two different sizes of structuring element. The experiment shows that the higher size of structuring element makes the image cleaner but changes the detected defects sequentially and makes the image unreal. Fig. 5c is observable as the best segmented result in Fig. 5.

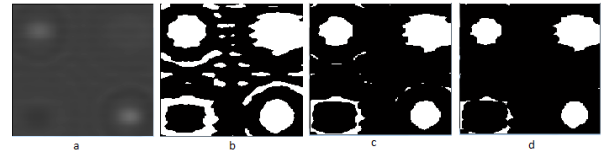


Fig. 5. Images of Sample 1 showing the total process of target segmentation using fuzzy c-mean clustering followed by multi-thresholding and erosion, a) original image b) fuzzy c-mean clustering, c) erosion by structuring element object 10 and d) erosion by structuring element object 15.

The comparison of segmentation results using the above three algorithms shows that the results achieved by ‘Algorithm 2’ (Fig. 4) outperform the other two algorithms. In Fig. 4, the best demonstration is for “cycling convolution of Gaussian as basis of Fourier transform” which is followed by multi-threshold segmentation method and morphological operation ‘erosion’. The image shows the clear view of four separated defects with less noise and redundant objects in an image.

In addition, Fig. 6 presents the surface plots for the magnitude and phase of reconstructed image based on wavelet transform and Fourier transform (Algorithm 1). The plots in the first row of Fig. 6 demonstrate the magnitude and phase of 2D- data containing random phases. The plots in the second row of Fig. 6 demonstrate the magnitude and phase of 2D-data containing random magnitude. According to the plots, although the second reconstruction is formed by the 2D-data with random magnitude, it is still more dominant than the reconstruction with random phase, while the later still provides distorted information. The second row in Fig.6 demonstrate the

magnitude and phase of 2D-data containing random magnitude.

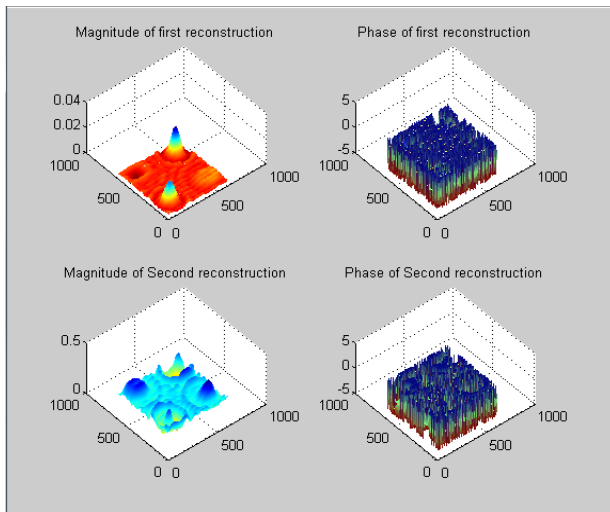


Fig. 6. A 3D demonstration of phase and magnitude of 2-D data (reconstructed image using wavelet)

Fig. 7 presents the surface plots for the magnitude and phase of reconstructed image based on Gaussian filtering and Fourier transform (Algorithm 2). The comparison of Fig. 6 and Fig. 7 shows that the phase in both rows of both Fig. 6 and Fig. 7 are still random, thus, showing the basis has little effect on phase, while the magnitude in first row of Fig. 6 has changed from  $[0, 0.03]$  by the wavelet basis to  $[0, 1]$  in first row of Fig. 7 by the Gaussian filtering. The magnitude in second row of Fig. 7 shows small changes compared to Fig. 6. This is obvious because the second row is the reconstructed image of 2D-data containing random magnitude which was described earlier.

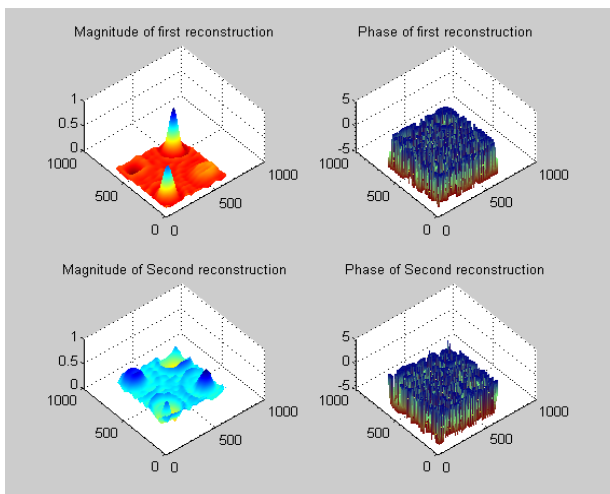


Fig. 7. A 3D demonstration of phase and magnitude of 2-D data (reconstructed image using Gaussian)

## V. CONCLUSION

The structuring of three algorithms for the defect segmentation of structures have been proposed. The algorithms

are based on the single and cyclic convolution of wavelet transform and Fourier transform, Gaussian filter and Fourier transform, and the last one, fuzzy c-mean clustering. Consequently, the algorithms were followed by multi-thresholding and morphological operation (erosion). The better segmentation results with less noise have been achieved by the cyclic convolution of Gaussian filter and Fourier transform followed by multi-thresholding and erosion.

Since there is no single best approach in image processing, the algorithms should be dictated by the problems at hand, by the methods being used, and by the results required. The proposed algorithms can easily be retargeted and investigated to apply in other domains of interest.

## REFERENCES

- [1] A.Qader, O. Abudayyeh, and M. Kelly, "Analysis of Edge-Detection Techniques for Crack Identification in Bridges." *J. Comput. Civ. Eng.*, vol. 17, no.4, pp. 255–263, 2003.
- [2] M. Pastorino, *Microwave imaging*, Hoboken, NJ, USA: Wiley, 2010.
- [3] S.S. Ahmed, A. Schiessl, F. Gumbmann, M. Tiebout, S. Methfessel, and L. Schmidt, "Advanced microwave imaging", *IEEE Microwave Magazine*, vol. 13, no. 6, pp. 26-43, 2012.
- [4] R. Zoughi, *Microwave nondestructive testing and evaluation*, Alphen aan den Rijn, The Netherlands: Kluwer, 2000.
- [5] S. Kharkovsky and R. Zoughi, "Microwave and millimeter wave nondestructive testing and evaluation - Overview and recent advances", *IEEE Instrum. Meas. Mag.*, vol. 10, no. 2, pp. 26-38, 2007.
- [6] M.T. Ghasr, M.A. Abou-Khousa, S. Kharkovsky, R. Zoughi and DF. Pommerenke, "Portable real-time microwave camera at 24 GHz", *IEEE Trans. Antennas Propag.*, vol. 60, no. 2, pp. 1114-1125, 2012.
- [7] H.Tanaka, M.Yamada, R. Sato, S. Hashimoto: Japanese Patent P2006-162477A, 2006.
- [8] T.C.Hutchinson and Z. Chen: "Improved image analysis for evaluating concrete damage", *J. Comput. Civil Eng.* vol. 20, no.3, pp. 210–216 2006.
- [9] A. Landstrom and M.J.Thurley, "Morphology-based crack detection for steel slabs", *IEEE Journal of selected topics in signal processing*, Vol.6, pp 866 – 875, 2012.
- [10] S. Iyer and S. K. Sinha, "Segmentation of pipe images for crack detection in buried sewers", *Comput. Aided Civil Infrastruct. Eng.* vol. 21, no.6, pp.395–410, 2006.
- [11] P. Cotić, E. Niederleithinger, V. Bosiljkov and Z. Jagličić, "NDT data fusion for the enhancement of defect visualization in concrete", *Key Engineering Materials*, vol. 569-570, pp. 175-182, 2013.
- [12] S. Kharkovsky, M.T. Ghasr, R. Ratnayake, B. Percy, "Microwave imaging with a 3-axis multifunctional scanning system," in *Proc IEEE Int. Instrum. Meas. Technol Conf. (I2MTC)*, pp. 1572-1575, 2014.
- [13] M. Grigoryan and S. S. Aghaian, "Tensor transform-based quaternion Fourier transform algorithm", *Information Sciences*, vol 320, no.1, pp. 62-74, 2015.
- [14] F.J. Narcowich and J.D. Ward, "Wavelets associated with periodic basis functions", *Appl. Comput. Harmon. Anal.*, vol. 3, pp. 40–56, 1996.